

$\text{Co}^{\text{III}}\text{Cl}_2$.^{23,24,26} It is possible that the disproportionation reaction is combined with chloride anion transformation as shown in reaction 4. The binding of a second chloride ion to the $\text{Co}(\text{III})$



center significantly reduces the $E_{1/2}$ for cation radical formation which occurs at 0.63 V as shown in Figure 5. The equilibrium constant for reaction 4 can thus be estimated as 3.6×10^{-7} . This corresponds to 0.12% species existing in either the cation radical state or the paramagnetic $\text{Co}(\text{II})$ state of the compound. A similar mechanism for the paramagnetic properties of $(\text{TPP})\text{Co}^{\text{III}}\text{Cl}$ has also been suggested.⁵

Acknowledgment. The support of the National Science Foundation (Grant No. CHE-8515411) is gratefully acknowledged. We also acknowledge Pierre-F. Blanchet for preliminary electrochemical results on reactions involving formation of (P)- $\text{Co}(\text{CH}_2\text{Cl})$.

Registry No. $(\text{TPP})\text{Co}$, 14172-90-8; $[(\text{TPP})\text{Co}]^-$, 31886-96-1; $[(\text{TPP})\text{Co}]^+$, 38414-01-6; $[(\text{TPP})\text{Co}]^{2+}$, 28132-69-6; $[(\text{TPP})\text{Co}]^{3+}$, 60430-19-5; $(\text{TPP})\text{CoCl}$, 60166-10-1; $[(\text{TPP})\text{CoCl}]^-$, 109123-05-9; $[(\text{TPP})\text{CoCl}]^+$, 109123-04-8; $(\text{TPP})\text{CoCl}_2$, 78992-04-8; $[(\text{TPP})\text{CoCl}_2]^-$, 109123-07-1; $(\text{TPP})\text{Co}(\text{CH}_3)$, 29130-60-7; $[(\text{TPP})\text{Co}(\text{CH}_3)]^-$, 109123-06-0; $(\text{TPP})\text{Co}(\text{CH}_2\text{Cl})$, 65856-25-9; Bu_4NCl , 1112-67-0; Cl , 16887-00-6; Bu_4NClO_4 , 1923-70-2.

Contribution from the Department of Chemistry, University of Houston, Houston, Texas 77004, and Laboratoire de Synthèse et d'Electrosynthèse Organométallique, Associé aux CNRS (UA 33), Faculté des Sciences "Gabriel", Université de Dijon, 21100 Dijon, France

Synthesis, Electrochemistry, and Ligand-Addition Reactions of Gallium(III) Porphyrins

K. M. Kadish,*^{1a} J.-L. Cornillon,^{1a} A. Coutsolelos,^{1b} and R. Guilard*^{1b}

Received March 2, 1987

The synthesis, electrochemistry, and ligand-addition reactions of ionic five- and six-coordinate gallium(III) porphyrins are reported. The reactions of *N*-methylimidazole and pyridine with (P) GaX , where P = the dianion of octaethylporphyrin (OEP) or tetraphenylporphyrin (TPP) and X = Cl^- , OAc^- , OH^- , or F^- , were monitored by ^1H NMR, electrochemistry, electronic absorption spectroscopy, and conductivity measurements. Results from all four methods were self-consistent and demonstrated the stepwise formation of hexacoordinated gallium porphyrin species of the type (P) GaX(L) and $[(\text{P})\text{Ga(L)}_2]^+$ where L = *N*-methylimidazole or pyridine. This is the first time that monomeric, hexacoordinated Ga(III) porphyrins have been reported. Equilibrium constants for ligand binding by (P) GaX and (P) GaX(L) were calculated from the electronic absorption spectra, and an overall oxidation/reduction mechanism is presented.

Introduction

It has been demonstrated that cofacially joined organometallic macrocyclic polymers such as $[\text{M}(\text{Pc})\text{O}]_n$ (where M = Si, Ge, or Sn and Pc = the dianion of phthalocyanine) give stable conducting materials after being partially oxidized with a variety of reagents.²⁻⁸ The isoelectronic group 13 polymers $[(\text{Pc})\text{AlF}]_n$ and $[(\text{Pc})\text{GaF}]_n$ can also be partially oxidized with I_2 ⁹ or nitrosoyl salts,^{10,11} and the resulting materials are highly conducting.

Variation of the central metal and the anionic bridging ligand in partially oxidized $[(\text{Pc})\text{MX}]_n$ structures may provide valuable insight into how in-plane ring spacing affects the electronic and optical properties of the complex. This was demonstrated for the case of partially oxidized $[(\text{Pc})\text{GaX}]_n$ and $[(\text{Pc})\text{AlX}]_n$, where X = Cl^- , Br^- , or I^- . The resulting complexes were partially oxidized with nitrosoyl salts and had a high conductivity.⁴

Variation of the macrocyclic ligand in the polymer may also lead to insights as to how the properties of the macrocycle affect the conducting properties of the complex, and the preparation of various precursors is of interest. In this regard, the synthesis¹² and characterization of gallium σ -bonded alkyl- and arylporphyrins and the bridge-stacked polymeric structure¹³ of a complex con-

taining fluorinated gallium(III) porphyrins have been published. The properties of the oxidized polymer are obviously related to the electrochemistry of the monomeric material, and the electrochemistry of σ -bonded gallium(III) porphyrins has also been published.¹⁴

This present article focuses on the synthesis, electrochemistry, and ligand-addition reactions of five- or six-coordinate gallium(III) porphyrins containing ionic axial ligands. The investigated complexes are represented by (P) GaX or (P) GaX(L) , where P is the dianion of tetraphenylporphyrin (TPP) or octaethylporphyrin (OEP), X = Cl^- , OAc^- , OH^- , or F^- , and L = H_2O . Some of these metalloporphyrins may be precursors for conductors, and it is thus of importance to have knowledge concerning the electrochemical properties and ligand-addition reactions of these monomeric complexes. The ligand-addition reactions were monitored by ^1H NMR and UV-visible spectroscopy, conductometry, and electrochemistry.

Experimental Section

Instrumentation. Electronic absorption spectra were taken by using a Perkin-Elmer 559 spectrophotometer, a Tracor Northern 1710 holographic optical spectrometer/multichannel analyzer, or an IBM 9430 spectrophotometer. IR spectra were obtained on a Perkin-Elmer 1330 spectrometer or a Perkin-Elmer 580B spectrometer. Samples were 1% dispersions in CsI or Nujol mulls. ESR spectra were recorded on an IBM Model ER 100D spectrometer equipped with an ER 40-X microwave bridge and an ER 080 power supply. ^1H NMR spectra were obtained on a Nicolet FT 300 or a JEOL FX-100 spectrometer. Samples were typically 3–4 mg in 0.5 mL of solvent, which was CD_2Cl_2 , CDCl_3 , C_6D_6 , or pyridine- d_5 . Mass spectra were recorded in the electron-impact mode on a Finnigan 3300 spectrometer. All spectra were obtained by direct inlet under the following conditions: electron impact; ionizing energy, 35–70 eV; ionizing current, 0.4 mA; source temperature, up to 250 °C.

Cyclic voltammograms were obtained with a three-electrode system. The working electrode was a platinum button and the counterelectrode a platinum wire. A saturated calomel electrode (SCE) served as a reference electrode and was separated from the bulk of the solution by a fritted glass bridge. An EG&G Model 173 potentiostat, an EG&G Model 175 universal programmer, and a Houston Instruments Model 200

- (1) (a) University of Houston, (b) Université de Dijon.
- (2) Nohr, R. S.; Kuznesof, P. M.; Wynne, K. J.; Kenney, M. E.; Siebenmann, P. G. *J. Am. Chem. Soc.* **1981**, *103*, 4371.
- (3) Diel, B. N.; Inabe, T.; Lyding, J. W.; Schoch, K. F.; Kannewurf, C. R.; Marks, T. J. *J. Am. Chem. Soc.* **1983**, *105*, 1539.
- (4) Nohr, R. S.; Wynne, K. J. *J. Am. Chem. Soc., Chem. Commun.* **1981**, 1210.
- (5) Swift, D. R. Ph.D. Dissertation, Case Western Reserve University, 1970.
- (6) Kroenke, W. J.; Sutton, L. E.; Joyner, R. D.; Kenney, M. E. *Inorg. Chem.* **1963**, *2*, 1064.
- (7) Esposito, J. N.; Lloyd, J. E.; Kenney, M. E. *Inorg. Chem.* **1966**, *5*, 1979.
- (8) Linsky, J. P.; Paul, T. R.; Nohr, R. S.; Kenney, M. E. *Inorg. Chem.* **1980**, *19*, 3131.
- (9) Petersen, J. L.; Schramm, C. S.; Stojakovic, D. R.; Hoffman, B. M.; Marks, T. J. *J. Am. Chem. Soc.* **1977**, *99*, 286.
- (10) Brant, P.; Nohr, R. S.; Wynne, K. J.; Weber, D. *Mol. Cryst. Liq. Cryst.* **1982**, *81*, 255.
- (11) Weber, D. C.; Brant, P.; Nohr, R. S.; Haupt, S. G.; Wynne, K. J. *J. Phys., Colloq. C-3* **1983**, *44*, Suppl. No. 6, 639.
- (12) Coutsolelos, A.; Guilard, R. *J. Organomet. Chem.* **1983**, *253*, 273.
- (13) Goulon, J.; Friant, P.; Goulon-Ginet, C.; Coutsolelos, A.; Guilard, R. *Chem. Phys.* **1984**, *83*, 367.

- (14) Kadish, K. M.; Boisselier-Cocolios, B.; Coutsolelos, A.; Mitaine, P.; Guilard, R. *Inorg. Chem.* **1985**, *24*, 4521.

Table I. Elemental Analyses and Mass Spectral Data

fragments	Mass Spectrometry ^a							
	(OEP)GaOH(H ₂ O)		(TPP)GaOH(H ₂ O)		(OEP)GaOAc		(TPP)GaOAc	
	m/e	rel intens, %	m/e	rel intens, %	m/e	rel intens, %	m/e	rel intens, %
[M + 2] ⁺	638	41.78	718	29.09				
[M + 1] ⁺	637	16.90	717	5.45	661	6.62	741	6.87
M ⁺	636	33.33			660	4.03	740	5.72
[M - H ₂ O + 2] ⁺	620	34.27	700	9.09				
[M - H ₂ O + 1] ⁺	619	12.20	699	3.63				
[M - H ₂ O] ⁺	618	21.12	698	10.90				
[(P)Ga + 2] ⁺	603	72.76	683	16.36				
[(P)Ga + 1] ⁺	602	47.88	682	30.90	602	100.00	682	93.51
[(P)Ga] ⁺	601	100.00	681	100.00	601	74.63	681	100.00
Analyses ^b (%)								
element	(OEP)GaOH(H ₂ O)		(TPP)GaOH(H ₂ O)		(OEP)GaOAc		(TPP)GaOAc	
C	67.6 (67.82)		73.7 (73.66)		68.9 (68.99)		74.4 (74.69)	
H	7.4 (7.43)		4.3 (4.36)		7.0 (7.16)		4.1 (4.22)	
N	8.7 (8.79)		7.7 (7.81)		8.1 (8.47)		7.4 (7.58)	
Ga	10.6 (10.93)		9.2 (9.72)		9.9 (10.54)		9.1 (9.43)	

^aRelative intensity of the peaks M⁺, (M + 1)⁺, and (M + 2)⁺ depends on the abundances of ⁶⁹Ga and ⁷¹Ga. ^bValues calculated are given in parentheses.

Table II. ¹H NMR Data for (P)GaOH(H₂O) and (P)GaOAc

compd	R ¹	R ²	bound anion	protons of R ¹		protons of R ²		protons of anion	
				n/i ^c	δ	n/i ^c	δ	n/i ^c	δ
(OEP)GaOH(H ₂ O) ^a	H	C ₂ H ₅	OH ⁻	s/4	10.55	t/24	1.93	s/1	-5.10
(TPP)GaOH(H ₂ O) ^a	C ₆ H ₅	H	OH ⁻	m/8 (o-H) m/12 (m, p-H)	8.26 7.80	s/8	9.19	s/1	-4.35
(OEP)GaOAc ^b	H	C ₂ H ₅	OAc ⁻	s/4	10.19	t/24	1.16	s/3	-1.42
(TPP)GaOAc ^b	C ₆ H ₅	H	OAc ⁻	m/8 (o-H) m/12 (m, p-H)	8.19 7.65	s/8	9.07	s/3	-0.75

^aSolvent = C₅D₅N. ^bSolvent = CDCl₃. ^cKey: n = number of lines, i = number of protons, s = singlet, t = triplet, m = multiplet.

X-Y recorder or a BAS-100 electrochemical analyzer and a HIPLOT DMP-40 plotter were used.

Controlled-potential electrolysis was performed with an EG&G Model 173 potentiostat or a BAS-100 electrochemical analyzer. Both the reference electrode and the platinum-wire counter electrode were separated from the bulk solution by means of a fritted-glass bridge.

Thin-layer spectroelectrochemical measurements were performed with an IBM EC 225 voltammetric analyzer coupled to a Tracor Northern 1710 holographic optical spectrometer/multichannel analyzer, which gave time-resolved spectral data. The utilized optically transparent thin-layer electrode (OTTLE) has been described in a previous publication.¹⁵

Ligand-addition reactions were monitored on an IBM 9430 spectrophotometer using matched quartz cells. An IBM PC/AT computer was used for calculating stability constants from the raw spectrophotometric data. Solution conductances were determined with a Metrohm AG Herisour Model EA 655 cell and a Model 31 YSI conductivity bridge. Measurements were taken at 20.0 ± 0.5 °C.

Chemicals. Tetrabutylammonium perchlorate ((TBA)ClO₄) (Fluka) was recrystallized twice from ethanol, dried, and stored under vacuum until use. Reagent grade methylene chloride (CH₂Cl₂) was distilled prior to use over CaH₂. N-Methylimidazole (N-MeIm) was vacuum-distilled and stored under argon. Pyridine (py) was refluxed over CaH₂ and then distilled prior to use over CaH₂ under a nitrogen atmosphere.

Synthesis of (P)GaCl and (P)GaAc. Two general methods were used to synthesize the gallium(III) porphyrins. The first uses NH₄Ga(SO₄)₂·12H₂O for metalation in acetic acid¹⁶ while the second uses Ga(acac)₃ for metalation in phenol.¹⁷ (P)GaCl has also been prepared by the reaction of GaCl₃ and (P)H₂ in acetic acid.¹⁸ About 3.5% of the free base is transformed into the corresponding (P)Ga(OAc) derivative when P = OEP or TPP.

In this study free base (OEP)H₂ or (TPP)H₂ (9.35 mmol) and GaCl₃ (13.63 mmol) were refluxed for 12 h in 425 mL of acetic acid containing

sodium acetate (61 mmol).^{18,19} The solution was cooled to 0 °C and the crystallized reaction product filtered. The solid was a mixture of (P)GaCl and small amounts of (P)GaOAc. This second complex was extracted from the filtrate with CH₂Cl₂ (400 mL) after neutralization with an aqueous solution of NaHCO₃ (5%, 400 mL). The solution was dried over MgSO₄, and after evaporation of the solvent, the precipitate was recrystallized by a 1:1 mixture of toluene/heptane. The yield of (OEP)GaOAc and (TPP)GaOAc was close to 3.5%.

Synthesis of (P)GaOH(H₂O). Synthesis of (P)GaOH(H₂O) was achieved by an anion-exchange reaction involving (P)GaCl, which was passed through a deactivated basic alumina column (eluent methanol: toluene) (1:10). This procedure has been described for the preparation of (P)TiOH(H₂O)^{20,21} and was also used for synthesis of the corresponding indium(III) porphyrins.²² The yield of the reaction and the solvent of recrystallization was as follows: (OEP)GaOH(H₂O), 50%, toluene; (TPP)GaOH(H₂O), 76%, toluene:heptane (1:1).

Synthesis of (P)GaF. The (P)GaF complexes were synthesized by reacting hydrofluoric acid in 40% water solutions with (P)GaCl in methanol.¹⁸

Results and Discussion

Chemical Characterization of the Gallium(III) Complexes. Elemental analysis and mass spectral data are given in Table I and suggest the formulas (P)GaOAc and (P)GaOH(H₂O). The molecular peak is present for most of these complexes, and the fragmentation patterns indicate the simultaneous elimination of a hydroxyl group and a water molecule. For all (P)GaX compounds the parent peak corresponds to the [(P)Ga]⁺ moiety (or the recombination ion [(P)GaH]⁺ in the case of (OEP)GaOAc).

¹H NMR data for (P)GaOAc and (P)GaOH(H₂O) are presented in Table II. The acetate and hydroxide derivatives exhibit

(15) Lin, X. Q.; Kadish, K. M. *Anal. Chem.* 1985, 55, 1498.

(16) Eaton, S. S.; Fishwild, D. M.; Eaton, G. R. *Inorg. Chem.* 1978, 17, 1542.

(17) Buchler, J. W.; Puppe, L. *Justus Liebigs Ann. Chem.* 1974, 1046.

(18) Coutsolelos, A.; Guillard, R.; Bayeul, D.; Lecomte, C. *Polyhedron* 1986, 5, 1157.

(19) Coutsolelos, A. These d'Etat, Université de Dijon, France, 1985.

(20) Abraham, R. J.; Smith, K. M. *Tetrahedron Lett.* 1971, 36, 3335.

(21) Abraham, R. J.; Barnett, G. H.; Smith, K. M. *J. Chem. Soc., Perkin Trans. 1* 1973, 2142.

(22) Cocolios, P.; Guillard, R.; Bayeul, D.; Lecomte, C. *Inorg. Chem.* 1985, 24, 2058.

Table III. Characteristic IR and UV–Visible Spectroscopic Data

complex	wavenumber, cm^{-1}	assignt	UV-visible ^a				
			B(1,0)	B(0,0)	Q(2,0)	Q(1,0)	Q(0,0)
(OEP)GaOAc	1663	$\nu_{as}(\text{C}=\text{O})$	377 (3.1)	397 (26.1)	488 (0.2)	531 (0.9)	568 (1.1)
	1270	$\nu_s(\text{C}=\text{O})$					
	340	$\nu(\text{Ga}=\text{O})$					
(TPP)GaOAc	1666	$\nu_{as}(\text{C}=\text{O})$	393 (20.7)	414 (132.8)		549 (7.4)	568 (3.3)
	1294	$\nu_s(\text{C}=\text{O})$					
	325	$\nu(\text{Ga}=\text{O})$					
(OEP)GaOH(H ₂ O)	3670	$\nu(\text{OH})$	376 (10.1)	395 (105.3)	494 (0.3)	550 (3.7)	568 (5.1)
	1659	$\delta(\text{H}_2\text{O})$					
	1059	$\delta(\text{Ga}=\text{OH})$					
	810	$\rho_r(\text{H}_2\text{O})$					
	601	$\rho_w(\text{H}_2\text{O})$					
	342	$\nu(\text{Ga}=\text{O})$					
(TPP)GaOH(H ₂ O)	3670	$\nu(\text{OH})$	396 (20.8)	414 (249.7)	512 (2.0)	549 (9.0)	589 (3.3)
	1688	$\delta(\text{H}_2\text{O})$					
	1088	$\delta(\text{Ga}=\text{OH})$					
	793	$\rho_r(\text{H}_2\text{O})$					
	619	$\rho_w(\text{H}_2\text{O})$					
	336	$\nu(\text{Ga}=\text{O})$					

^a Values given are of λ (nm) with $\epsilon (10^3 \times M^{-1} \text{ cm}^{-1})$ in parentheses. Solvent CH₃OH.

spectral characteristics of diamagnetic complexes. The morphology of the (P)GaOAc resonance signals is very simple. For (OEP)GaOAc, the meso protons appear as a singlet at 10.19 ppm and the anisochrony of methylenic protons of C₂H₅ group is typical of a pentacoordination scheme. Resonances of pyrrolic and ortho, meta, and para hydrogens appear at 9.07, 7.65 (*m*, *p*-H), and 8.19 ppm (*o*-H) for (TPP)GaOAc. The protons of the axial carboxylate group of the OEP and TPP derivatives appear as a singlet close to -1.42 and -0.75 ppm, respectively.

The NMR spectra of (P)GaOH(H₂O) have the same morphology in pyridine-*d*₅ and are similar to those of the acetate complexes (see Table II). However, two differences can be discussed. First, a broad peak due to the OH⁻ anion appears at -5.10 ppm for (OEP)GaOH(H₂O) and -4.35 ppm for (TPP)GaOH(H₂O) in pyridine-*d*₅. This is shown in Figure 1 where the ¹H NMR spectra of (OEP)GaOH(H₂O) in pyridine-*d*₅ are represented before and after addition of D₂O. After addition of D₂O the signal close to 5 ppm disappears. This can be attributed to the exchange of hydrogen by deuterium atoms in solution. Second, the methylenic protons of the (OEP)GaOH(H₂O) are pseudoisochronous, implying a trans configuration of OH⁻ and second axial ligand. The fact that a water molecule on (OEP)GaOH(H₂O) has been replaced by pyridine-*d*₅ is demonstrated by the NMR spectrum in C₆H₆. The NMR spectra of (OEP)GaOH(H₂O) in C₆D₆ and C₆D₅N exhibit the same morphology (meso protons, 10.36 ppm; pseudoisochronous methylene protons, 3.97 ppm; methyl protons, 1.84 ppm), but the resonance signal of the OH⁻ ligand in C₆D₆ appears at -6.81 ppm as compared to -5.10 ppm in C₆D₅N. This difference in the OH⁻ resonance implies that the H₂O ligand is replaced by pyridine-*d*₅ to form the six-coordinate complex.

Table III lists the characteristic IR and UV–Visible data of the (P)GaOAc and (P)GaOH(H₂O) complexes. As shown in this table the $\nu(\text{CO}_2^-)$ stretching frequencies are observed at 1663 and 1270 cm⁻¹ for the OEP complex and at 1666 and 1294 cm⁻¹ for the TPP complex. The values of the frequency difference ($\Delta\nu = 393 \text{ cm}^{-1}$ for the OEP complex and $\Delta\nu = 372 \text{ cm}^{-1}$ for the TPP complex) exclude bis ligation.^{23,24} Moreover, a band of low intensity appears in the region 325–340 cm⁻¹. This absorption is attributable to the Ga–O vibration.

Hydroxyl group stretching frequencies of hydroxy complexes appear in the range 3580–3640 cm⁻¹.^{23,24} Broad peaks resulting from hydrogen bonding have been reported between 3580 and 3700 cm⁻¹ for the (P)TiOH(H₂O) complexes.^{18,19} The (P)InOH(H₂O)

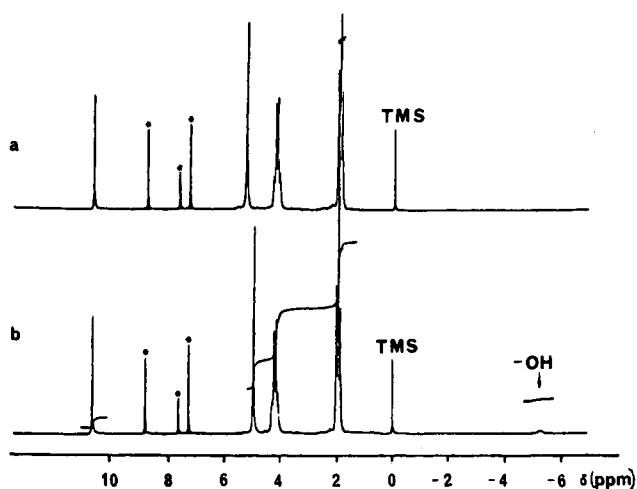


Figure 1. ¹H NMR spectra of (TPP)GaOH(H₂O) in pyridine-*d*₅: (a) after addition of D₂O; (b) before addition of D₂O.

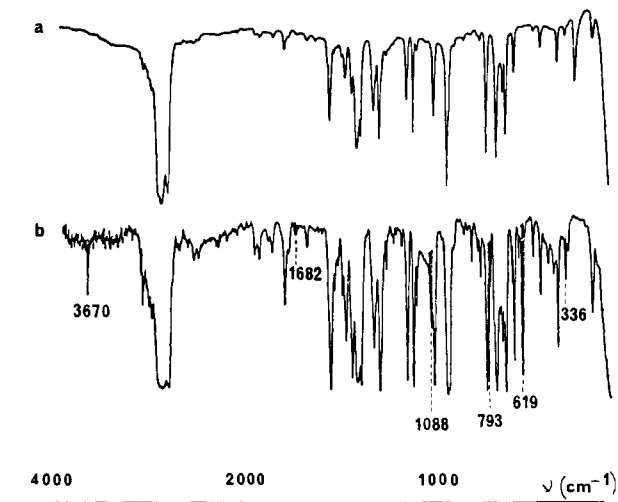


Figure 2. IR spectra in Nujol: (a) (TPP)GaCl; (b) (TPP)GaOH(H₂O).

derivatives show a broad vibration at about 3630 cm⁻¹.²⁰ The (P)GaOH(H₂O) complex has a sharp peak at about 3670 cm⁻¹ (see Figure 2 and Table III). Two weak peaks are also seen close to 350 cm⁻¹ and are attributed to the gallium–oxygen stretching frequencies.^{23,24} The GaOH bending mode is observed at 1059 and 1088 cm⁻¹, respectively, for the OEP and TPP derivatives.

(23) Nakamoto, K. In *Infrared and Raman Spectra of Inorganic and Coordination Compounds*; Wiley: New York, 1978; p 226.

(24) Maslowksy, E., Jr. In *Vibrational Spectra of Organometallic Compounds*; Wiley: New York, 1977, p 186.

Table IV. Half-Wave Potentials (V vs. SCE) of (P)GaX and (P)GaOH(H₂O) in CH₂Cl₂ Containing 0.1 M (TBA)ClO₄

P ^b	X ^{-b}	oxidn		redn	
		2nd	1st	1st	2nd
TPP	Cl ⁻	1.40	1.16	-1.12	-1.52
	OAc ⁻	1.41	1.17	-1.14	-1.53
	F ⁻	1.42	1.18	-1.15	-1.54
	OH ⁻		1.17	-1.16	-1.54
OEP	Cl ⁻	1.44	1.00	-1.38	-1.81
	OAc ⁻	1.44	1.01	-1.36	-1.87 ^a
	F ⁻	1.45	1.00	-1.38	-1.82
	OH ⁻	1.44	1.01	-1.37	-1.88 ^a

^a E_p at 100 mV/s. ^b P = porphyrin macrocycle; X⁻ = anion.

In addition, all of the stretching frequencies in Table III correspond to complexes that have a water molecule axially coordinated to the complex. In summary, the spectroscopic data agree well with mono ligation for (P)GaOAc and with bis ligation for (P)GaO(H₂O).

Electrochemistry and Spectroelectrochemistry of (P)GaX in Nonbonding Solvents. The electrochemistry of (P)GaX and (P)GaOH(H₂O) is straightforward and is not unlike the electrochemistry of other group 13 metalloporphyrins in nonbonding solvents.^{14,25,26} Each Ga(III) complex shows two reversible oxidations and two reversible reductions within the solvent potential window. The diagnostic criteria developed by Fuhrhop et al.²⁷ for ring centered oxidation and reduction reactions is followed for these complexes ($E_{1/2}(\text{oxidn}) - E_{1/2}(\text{redn}) = 2.25 \pm 0.15$ V, $\Delta E_{1/2}(\text{redn}) = 0.42 \pm 0.05$ V, and $\Delta E_{1/2}(\text{oxidn}) = 0.29 \pm 0.05$ V) and both π -anion radicals and π -cation radicals can be postulated to form after oxidation or reduction of each complex. Table IV summarizes half-wave potentials for these reactions in CH₂Cl₂ containing 0.1 M (TBA)ClO₄.

Thin-layer spectra were recorded during the first reduction and the first oxidation of (P)GaX and (P)GaOH(H₂O). The resulting electronic absorption spectra are characteristic of anion or cation radicals after the abstraction or addition of one electron to the complex. An example of the obtained thin-layer spectra is shown in Figure 3 for (OEP)GaOAc in CH₂Cl₂ containing 0.1 M (TBA)ClO₄, and spectral data for all of the singly oxidized and singly reduced Ga(III) complexes are summarized in Table V.

ESR spectra were also recorded after the addition and abstraction of one electron to (P)GaX. In all cases the spectra exhibited an ESR signal centered at g = 2.00. The singly reduced species were ESR active only at low temperature, and no ESR signal was recorded at room temperature. However, the singly oxidized species exhibited an ESR signal at both room temperature and low temperature.

The room-temperature signal of [(TPP)GaX]⁺ consists of four well-defined lines due to a small coupling with the gallium atom ($A = 10$ G, corresponding to about 0.3% spin density on Ga). The origin of the metal interaction ($I_{\text{Ga}} = 3/2$) for [(TPP)GaX]⁺ is identical with that which has been proposed for cobalt,^{28,29} zinc,³⁰⁻³² indium,²⁶ and thallium³³ porphyrins and arises from a σ - π spin-polarization mechanism.

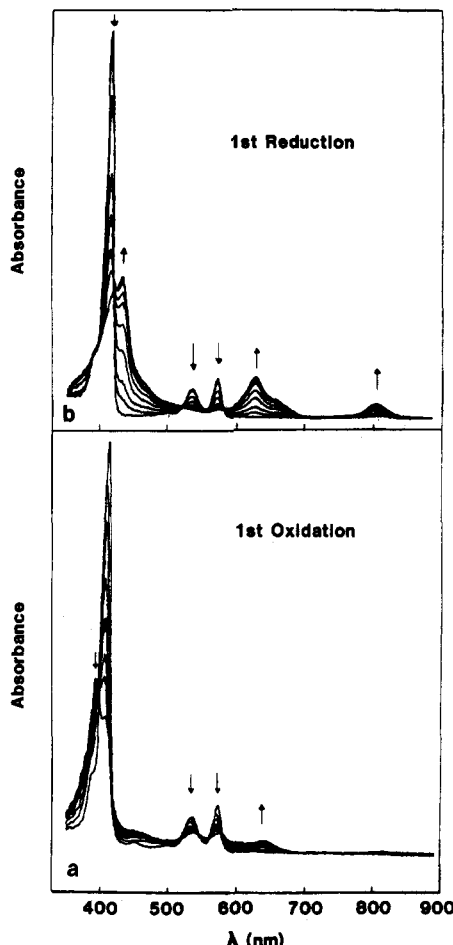


Figure 3. Thin-layer spectral changes for (OEP)GaOAc in CH₂Cl₂ containing 0.1 M (TBA)ClO₄: (a) during the first oxidation; (b) during the first reduction.

Table V. Maximum Absorbance Wavelengths (λ_{max}) and Corresponding Molar Absorptivities (ϵ) of Neutral, Singly Reduced, and Singly Oxidized (P)GaX and (P)GaOH(H₂O) in CH₂Cl₂ Containing 0.1 M (TBA)ClO₄

P ^a	X ^{-a}	electrode reacn	λ_{max} , nm ($10^3 \epsilon$, M ⁻¹ cm ⁻¹)		
			none	oxidn	redn
TPP	Cl ⁻	none	420 (620.1)	552 (22.4)	587 (5.9)
		oxidn	415 (205.4)	459 (39.3)	510 (11.4)
		redn	452 (240.3)	715 (24.2)	870 (17.8)
	OAc ⁻	none	419 (624.3)	552 (21.9)	586 (5.8)
		oxidn	416 (203.7)	460 (40.1)	609 (12.1)
		redn	451 (241.4)	718 (28.7)	872 (17.1)
	F ⁻	none	420 (632.3)	553 (22.4)	586 (5.80)
		oxidn	416 (204.5)	459 (38.4)	610 (10.9)
		redn	453 (235.6)	715 (28.9)	870 (18.4)
	OH ⁻	none	421 (621.7)	553 (22.0)	586 (5.4)
		oxidn	415 (200.1)	459 (38.3)	610 (10.5)
		redn	452 (234.4)	715 (27.5)	870 (17.4)
OEP	Cl ⁻	none	409 (375.4)	535 (17.0)	573 (23.9)
		oxidn	395 (290.4)	545 (17.4)	645 (18.3)
		redn	428 (230.3)	628 (23.4)	808 (9.0)
	OAc ⁻	none	408 (349.7)	536 (16.4)	573 (21.8)
		oxidn	395 (284.6)	546 (15.3)	646 (16.4)
		redn	428 (231.0)	628 (21.3)	808 (8.4)
	F ⁻	none	409 (370.3)	535 (16.8)	574 (22.4)
		oxidn	396 (287.4)	549 (16.4)	574 (20.9)
		redn	429 (225.4)	629 (21.8)	808 (7.9)
	OH ⁻	none	408 (367.4)	537 (15.9)	573 (22.0)
		oxidn	395 (280.9)	540 (14.9)	646 (15.8)
		redn	428 (224.8)	628 (20.9)	808 (9.0)

^a P = porphyrin macrocycle; X⁻ = anion.

- (25) Kadish, K. M.; Boisselier-Cocolios, B.; Cocolios, P.; Guillard, R. *Inorg. Chem.* **1985**, *24*, 2139.
- (26) Kadish, K. M.; Cornillon, J.-L.; Cocolios, P.; Tabard, A.; Guillard, R. *Inorg. Chem.* **1985**, *24*, 3645.
- (27) Fuhrhop, J.-H.; Kadish, K. M.; Davis, D. G. *J. Am. Chem. Soc.* **1973**, *95*, 5140.
- (28) Fajer, J.; Davis, M. S. In *The Porphyrins*; Dolphin, D., Ed.; Academic: New York, 1978; Vol. IV, Chapter 4 and references therein.
- (29) Wolberg, A.; Manassen, J. *J. Am. Chem. Soc.* **1966**, *88*, 1113.
- (30) Fajer, J.; Borg, D. C.; Forman, A.; Dolphin, D.; Felton, R. M. *J. Am. Chem. Soc.* **1970**, *92*, 3451.
- (31) Fajer, J.; Borg, D. C.; Forman, A.; Adler, A. D.; Varadi, V. *J. Am. Chem. Soc.* **1974**, *96*, 1238.
- (32) Fajer, J.; Borg, D. C.; Forman, A.; Felton, R. H.; Vehg, C.; Dolphin, D. *Ann. N.Y. Acad. Sci.* **1973**, *206*, 349.
- (33) Mengersen, C.; Subramanian, J.; Fuhrhop, J. M.; Smith, K. M. *Z. Naturforsch., A: Phys., Phys. Chem., Kosmophys.* **1974**, *29A*, 1827.

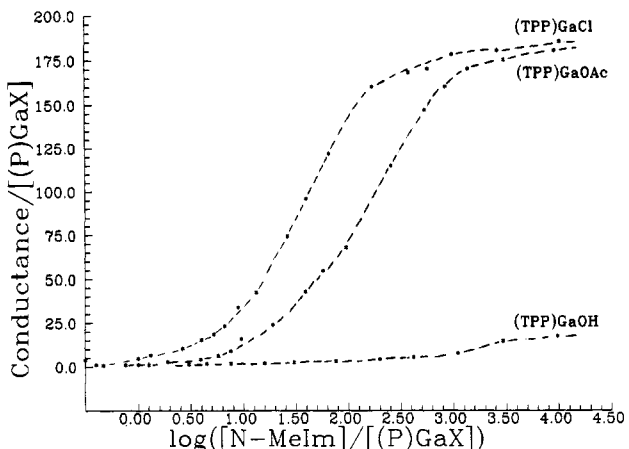


Figure 4. Conductivity of (OEP)GaX complexes in $\text{CH}_2\text{Cl}_2/\text{N-MeIm}$ mixtures.

N-Methylimidazole and Pyridine Addition to (P)GaOH(H_2O). Figure 4 illustrates the conductivity of (P)GaCl, (P)GaOAc, and (P)GaOH(H_2O) in CH_2Cl_2 containing increasing concentrations of N-methylimidazole. The conductance/porphyrin concentration ratio maximum is close to that obtained for a 1:1 electrolyte such as (TBA) ClO_4 or (TBA) PF_6 under the same experimental conditions and indicates a dissociation of the Ga-Cl and Ga-OAc bonds in the presence of excess N-MeIm. However, no dissociation of OH^- from (TPP)GaOH(H_2O) is observed up to 40 000 equiv of N-MeIm.

A similar behavior was observed for (TPP)GaF, which also did not show dissociation of F^- . When py was used as the complexing ligand only (P)GaCl was dissociated in solution and neither (P)GaOAc, (P)GaF, nor (P)GaOH(H_2O) exhibited any conductivity. This data reflects differences in the ionic Ga-X bond strength in the presence of N-MeIm and py and suggests that the Ga-X bond strength increases with X as follows: $\text{Cl}^- < \text{OAc}^- < \text{F}^- \approx \text{OH}^-$.

Figure 5a shows changes that occur in the electronic absorption spectra of (TPP)GaOH(H_2O) during a titration with N-MeIm in CH_2Cl_2 containing 0.1 M (TBA) ClO_4 . ((TBA) ClO_4 was added in order to more closely approximate the solution conditions where electrochemistry was carried out). As seen in Figure 5, there is a red shift in the Soret and Q bands upon complexation. The Q bands of (TPP)GaOH(H_2O) also change in relative intensity upon binding of N-MeIm. Four isobestic points are observed at 421, 556, 579, and 588 indicating the presence of only two species in solution.

Similar spectra changes occurred during titrations of the other (P)GaX complexes with N-MeIm, and at least three isobestic points were obtained in each case. A logarithmic analysis of the spectral changes were performed and for each complex gave a straight line slope of 1.0 (see Figure 5b), thus indicating the addition of only one N-MeIm molecule to (TPP)GaX.³⁴

Table VI summarizes stability constants for the addition of N-MeIm and py to (P)GaX. The conductivity data indicate that (P)GaF and (P)GaOH(H_2O) do not dissociate in $\text{CH}_2\text{Cl}_2/\text{N-MeIm}$ or $\text{CH}_2\text{Cl}_2/\text{py}$ mixtures nor does (P)GaOAc dissociate in solutions of CH_2Cl_2 and py. Therefore, the spectral indicate observed during titration of those complexes suggests the formation of (P)GaX(L) as shown by eq 1, where L = H_2O or no ligand.



The calculated stability constant for addition of one N-MeIm molecule to (TPP)GaCl is $10^{4.7}$ and implies that the reaction is over 99% shifted to the right at a ligand:porphyrin ratio of 5. No conductivity of the complex is observed at this ratio (see Figure 4), thus implying the formation of (P)GaX(L) and not [(P)Ga(X(L))₂]⁺ Cl^- .

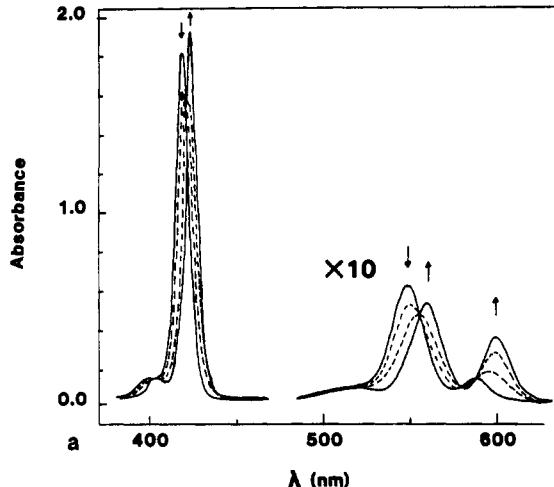


Figure 5. (a) Changes observed in the electronic absorption spectra of (TPP)GaOH(H_2O) in CH_2Cl_2 containing 0.1 M (TBA) ClO_4 during a titration with N-MeIm. (b) log-log analysis of the resulting spectral changes.

Table VI. Stability Constants ($\log K_1^a$) for Addition of N-Methylimidazole and Pyridine to (P)GaX and (P)GaOH(H_2O) in CH_2Cl_2 Containing 0.1 M (TBA) ClO_4

P ^b	X ^{-b}	ligand	
		N-MeIm	py
TPP	Cl ⁻	4.7	2.5
	OAc ⁻	4.0	1.7
	F ⁻	3.6	1.3
	OH ⁻	3.8	1.4
OEP	Cl ⁻	4.3	2.4
	OAc ⁻	3.7	1.7
	F ⁻	3.3	1.4
	OH ⁻	3.4	1.5

^a Values of $\log K_1$ good to ± 0.3 . ^b P = porphyrin macrocycle; X⁻ = anion.

Large spectral changes occur after the first ligand addition to (P)GaX or (P)GaOH(H_2O), and no further spectral changes are observed even at very high ligand concentrations. This is in contrast to (P)InX, where very small differences are observed in electronic absorption spectra after the addition of one N-MeIm to (P)InX³⁵ and dramatic spectral changes only occur after addition of a second ligand to give [(P)In(L)₂]⁺. These differences between (P)GaX(L) and (P)InX(L) spectra can be rationalized by the different sizes of In(III) (0.81 Å) and Ga(III) (0.62 Å).³⁶ The Ga(III) ion is small enough so that it will fit into the porphyrin

(35) Cornillon, J.-L.; Anderson, J. E.; Kadish, K. M. *Inorg. Chem.* 1986, 25, 991.

(36) *Handbook of Chemistry and Physics*, 66th ed.; CRC: New York, 1985.

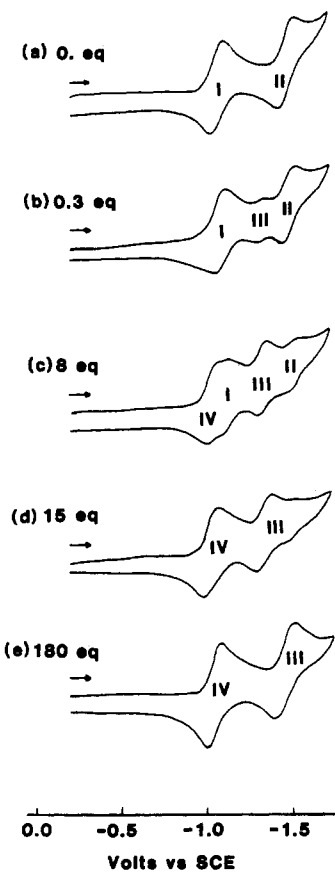


Figure 6. Cyclic voltammograms of (TPP)GaCl in 0.1 M (TBA)ClO₄ containing the following equivalents of *N*-MeIm: (a) 0; (b) 0.3; (c) 8; (d) 15; (e) 180.

plane after coordination of one ligand molecule. In contrast, the In(III) moves into the porphyrin plane only after complete replacement of the ionic ligand³⁷ and formation of [(P)In(L)₂]⁺ in solution.

The binding of *N*-MeIm by (OEP)GaCl was monitored by ¹H NMR spectroscopy. Addition of 1.5 equiv of *N*-MeIm to (OEP)GaCl leads to a 3 ppm upfield shift of the *N*-MeIm protons compared to free *N*-MeIm. This upfield shift indicates coordination of *N*-MeIm to the gallium complex. Further addition of *N*-MeIm leads to a downfield shift of the *N*-MeIm protons and changes the morphology of the signal arising from the α -CH₂ protons from an ABX₃ type to an A₂X₃ type. A similar behavior was observed for (OEP)InSO₃Ph(*N*-MeIm) and [(OEP)In(*N*-MeIm)₂]⁺ formation in solution.³⁵

The same explanation can be given for the ¹H NMR data on (OEP)GaCl. The reaction of (OEP)GaOAc with *N*-MeIm leads to the same shifts in the ¹H NMR signals. However, at high *N*-MeIm concentrations, the signal arising from OAc⁻ (-1.42 ppm in neat C₆D₆) is shifted downfield, indicating a dissociation of this group from [(P)Ga]⁺.

Electrochemistry in CH₂Cl₂/N-MeIm Mixtures. An electrochemically monitored titration of (TPP)GaCl with *N*-MeIm in CH₂Cl₂ containing 0.1 M (TBA)ClO₄ is shown in Figure 6. Two reversible one-electron reductions are observed at $E_{1/2} = -1.12$ (process I) and -1.52 V (process II) in the absence of *N*-MeIm. The addition of 0.3 equiv of *N*-MeIm to this solution leads to the appearance of a new process (labeled wave III) at $E_{1/2} \approx -1.3$ V. Further addition (8 equiv) leads to a new reduction wave (labeled wave IV), which is at a more positive potential than wave I and does not shift as a function of [*N*-MeIm]. Additional increases in the *N*-MeIm concentration from 15 to 180 equiv leads

Table VII. Half-Wave Potentials (V vs. SCE) for the Reduction of (P)GaX and (P)GaOH(H₂O) in Pyridine and CH₂Cl₂/N-MeIm Mixtures Containing 0.1 M (TBA)ClO₄

P ^c	X ^{-c}	py		1 M N-MeIm	
		1st	2nd	1st	2nd
TPP	Cl ⁻	-0.86	-1.40	-1.06	-1.52
	OAc ⁻	-1.10 ^a -0.85 ^b	-1.40	-1.06	-1.51
	OH ⁻	-1.15	-1.55	-1.15	-1.55
	F ⁻	-1.15	-1.55	-1.16	-1.54
OEP	Cl ⁻	-1.15	-1.70	-1.24	-1.77
	OAc ⁻	-1.35 ^a -1.16 ^b	-1.70	-1.29 ^b	-1.77
	OH ⁻	-1.38	-1.82	-1.38	-1.82
	F ⁻	-1.38	-1.81	-1.37	-1.82

^a E_{pa} at 100 mV/s (see text for mechanistic detail). ^b E_{pc} at 100 mV/s (see text for mechanistic detail). ^c P = porphyrin macrocycle; X⁻ = anion.

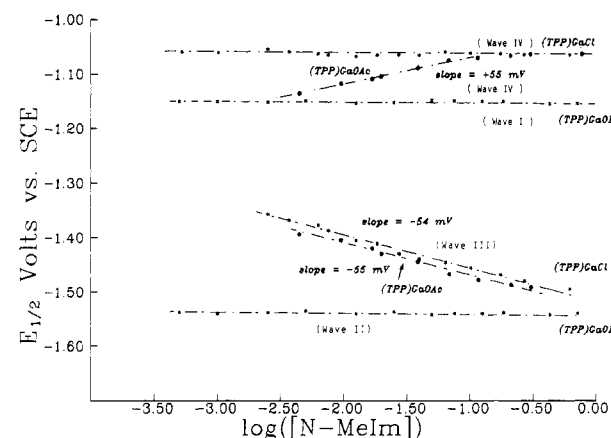
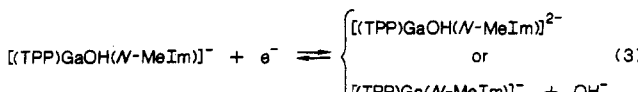
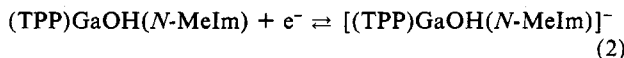


Figure 7. Dependence of $E_{1/2}$ on *N*-MeIm concentration for the reduction of (TPP)GaX and (TPP)GaOH(H₂O) complexes in CH₂Cl₂.

to the complete disappearance of the original processes I and II and to complete formation of the new waves III and IV, the first of which shifts toward more negative potentials with an increase in the ligand concentration. The potentials in CH₂Cl₂ containing 0.1 M (TBA)ClO₄ and 1 M *N*-methylimidazole are listed in Table VII.

Similar titrations were carried out with the other (P)GaX and (TPP)GaOH(H₂O) complexes, and the measured $E_{1/2}$ values are shown in Figure 7 as a function of the *N*-MeIm concentration for (TPP)GaCl, (TPP)GaOAc, and (TPP)GaOH(H₂O). New waves appear during the titration of (TPP)GaCl and (TPP)GaOAc, but in the case of (TPP)GaOH(H₂O), only the original two reductions are observed at all concentrations of *N*-MeIm. Each of the reduction potentials in 1 M *N*-MeIm is listed in Table VII.

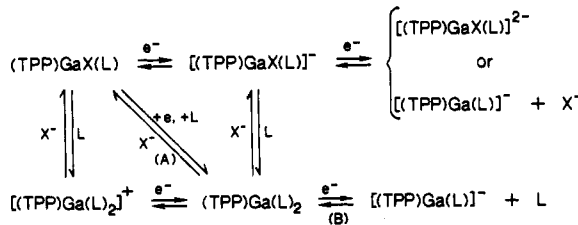
The electrochemical behavior of the different (P)GaX complexes parallels differences reported by conductimetry and spectroscopy. Half-wave potentials for reduction of (TPP)GaOAc(H₂O) are independent of the *N*-MeIm concentration over the range of 10⁻³ to 1 M and suggest the electrode reactions given by eq 2 and 3.



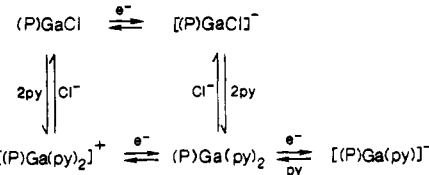
The theoretical shift of $E_{1/2}$ with changes of ligand binding is observed for waves I and II of (TPP)GaCl (see Figures 6 and 7). $E_{1/2}$ for the first reduction is independent of the *N*-MeIm concentration while $E_{1/2}$ for the second reduction shifts by -55 mV per 10-fold increase in *N*-MeIm concentration. This shift indicates the loss of one *N*-MeIm molecule after the second electron

(37) A difference in the M-Cl bond strength cannot account for the difference in reactivity since a simple computation from IR data leads to a stretching force constant ratio of 1.0.

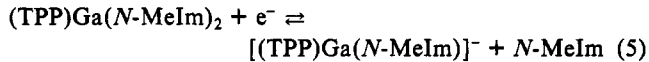
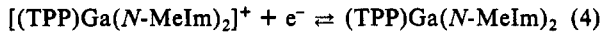
Scheme I



Scheme II



transfer.³⁸ The conductivity studies and the electronic absorption spectra show that (TPP)GaCl(*N*-MeIm) is readily formed after 1 equiv of *N*-MeIm is added to (TPP)GaCl solutions and that [(TPP)Ga(*N*-MeIm)₂]⁺Cl⁻ is the ultimate product at more than 150 equiv of *N*-MeIm. Thus, the $E_{1/2}$ dependence on ligand concentration for waves I and II can be explained by eq 4 and 5. These reactions are similar to what is observed for (P)InSO₃Ph reduction in the same solvent system.



The electrochemical behavior of (TPP)GaOAc is intermediate between that of (TPP)GaCl and that of (TPP)GaOH(H₂O). At log [N-MeIm] values between -2.2 and -1.0 the first reduction shifts positively by 55 mV per 10-fold increase in log [N-MeIm] while the second reduction shifts negatively by 54 mV per 10-fold increase in ligand concentration. This implies the gain of one *N*-MeIm molecule after the first reduction and the loss of one ligand after the second reduction. $E_{1/2}$ for the first reduction does not shift at log [N-MeIm] values greater than -1.0, and the potential is identical with that for the first reduction of (TPP)GaCl under the same conditions. However, at the same time the second reduction still shifts by -54 mV per 10-fold increase in *N*-MeIm concentration. Identical results were obtained for (TPP)GaX and (TPP)GaX(L), and Scheme I summarizes the various electrode reactions of these complexes in the presence of *N*-MeIm, which is identified as L.

Only the upper part of Scheme I is followed when X = OH⁻ or F⁻. When X = OAc⁻ the electron transfers occur through paths A and B at log [N-MeIm] between -2.2 and -1.0 but for log [N-MeIm] greater than -1.0 the reduction occurs via the lower pathway in Scheme I. The electrode reactions also occur as shown in Scheme I for (TPP)GaCl, (OEP)GaX, and (TPP)GaOH(H₂O).

Electrochemistry of (P)GaX, Where X = Cl⁻, OH⁻, and F⁻, in CH₂Cl₂/Pyridine and Neat Pyridine Mixtures. Similar results are obtained when py is added to (P)GaX solutions as in the case of *N*-methylimidazole addition to (P)GaX. A similar set of electrode reactions is also observed for (P)GaX and (P)GaOH(H₂O) in CH₂Cl₂/py or CH₂Cl₂/*N*-MeIm mixtures.

(P)GaOAc exhibits electrochemical behavior identical with that of (P)InCl³⁹ where the reduction mechanism shown in Scheme II occurs in the presence of pyridine. The electrochemistry of (P)GaOAc in CH₂Cl₂/py mixtures or neat pyridine is in agreement with Scheme II. Scan rate studies in pyridine show that the first reduction peak and its back-oxidation peak shift by -30

- (38) Crow, D. R. In *Polarography of Metal Complexes*; Academic: London, 1969.
 (39) Cornillon, J.-L.; Anderson, J. E.; Kadish, K. M. *Inorg. Chem.* 1986, 25, 2611.

and +30 mV per 10-fold increase of the scan rate, respectively. This indicates a chemical reaction following the electron transfer⁴⁰ and agrees with the "box mechanism" in Scheme II. Furthermore, both (P)GaCl and (P)GaOAc exhibit a second reduction at the same $E_{1/2}$ value in neat py (see Table VII), showing that the same redox couple is involved for the second reduction. This reaction is (P)Ga(py)₂/[(P)Ga(py)]⁻.

In conclusion, we have shown that hexacoordinated gallium(III) porphyrins are formed upon reaction with nitrogenous bases such as pyridine and *N*-MeIm. This agrees with the isolation of (TPP)GaCl(py) in the solid state. When the anionic ligand on (P)GaX is Cl⁻ or OAc⁻, either (P)GaX(L) or [(P)Ga(L)₂]⁺X⁻ is formed depending upon the concentration of the nitrogenous base. However, the (TPP)GaOH(H₂O) and (P)GaF complexes form only the mono *N*-MeIm adduct. Similar differences between chloro and fluoro derivatives have already been observed for iron porphyrins.⁴¹ For instance, the formation of [(TPP)Fe(DMSO)₂]⁺ is observed when (TPP)FeCl is dissolved in DMSO.⁴¹ This is in contrast to (TPP)FeF, which does not dissociate in DMSO solution and forms only (TPP)FeF(DMSO) in DMSO.⁴¹

The addition of one or two nitrogenous bases to (P)GaX, where X⁻ = Cl⁻ or OAc⁻, leads to dramatic changes in the electrochemistry. Shifts of 150–200 mV are observed in $E_{1/2}$. However, almost no changes are observed for (P)GaX when X = OH⁻ or F⁻. The results obtained for (P)GaOH(H₂O) have led to interesting structural implications.

(P)GaOH(H₂O) has a solvated water molecule similar to (P)Ti(OH)^{18,19} and (P)InOH.²⁰ This was shown unambiguously by IR and mass spectroscopy. Moreover, the spectroscopic data are in good agreement with a trans coordination of OH⁻ and H₂O although no X-ray structure is available. We have shown that either py or *N*-MeIm binds readily with (P)GaOH(H₂O) to form the hexacoordinated complex. If the water molecule is trans to OH⁻, this implies an easy displacement of H₂O by either py or *N*-MeIm, indicating a weak interaction.

Acknowledgment. The support of the National Science Foundation (Grants CHE-8515411 and INT-8413696) and the CNRS is gratefully acknowledged.

Registry No. [(TPP)GaCl]²⁻, 109907-38-2; [(TPP)GaCl]⁻, 98943-21-6; (TPP)GaCl, 78833-52-0; [(TPP)GaCl]⁺, 98943-44-3; [(TPP)GaCl]²⁺, 109907-31-5; [(TPP)GaOAc]²⁻, 109907-39-3; [(TPP)GaOAc]⁻, 109907-20-2; (TPP)GaOAc, 105796-33-6; [(TPP)GaOAc]⁺, 109907-19-9; [(TPP)GaOAc]²⁺, 109907-32-6; [(TPP)GaF]²⁻, 109907-40-6; [(TPP)GaF]⁻, 109907-22-4; (TPP)GaF, 104453-20-5; [(TPP)GaF]⁺, 109907-21-3; [(TPP)GaF]²⁺, 109907-33-7; [(TPP)GaOH(H₂O)]²⁻, 109907-41-7; [(TPP)GaOH(H₂O)]⁻, 109907-24-6; (TPP)GaOH(H₂O), 109907-17-7; [(TPP)GaOH(H₂O)]⁺, 109907-23-5; (TPP)GaOAc(py), 109907-46-2; [(TPP)GaF(N-MeIm)]⁻, 109907-59-7; (TPP)GaF(N-MeIm), 109907-47-3; (TPP)GaF(py), 109907-48-4; [(TPP)GaOH(N-MeIm)]⁻, 109907-55-3; (TPP)GaOH(N-MeIm), 109907-49-5; (TPP)GaOH(py), 109907-50-8; [(TPP)Ga(N-MeIm)]⁻, 109907-58-6; (TPP)Ga(N-MeIm)₂, 109907-57-5; [(TPP)Ga(N-MeIm)₂]⁺, 109907-56-4; [(TPP)Ga(py)]⁻, 109907-68-8; (TPP)Ga(py)₂, 109907-66-6; [(TPP)Ga(py)₂]⁺, 109927-21-1; [(OEP)GaCl]²⁻, 109907-42-8; [(OEP)GaCl]⁻, 98943-22-7; (OEP)GaCl, 87607-70-3; [(OEP)GaCl]⁺, 98943-52-3; [(OEP)GaCl]²⁺, 109907-34-8; [(OEP)GaOAc]²⁻, 109907-43-9; [(OEP)GaOAc]⁻, 109907-26-8; (OEP)GaOAc, 105796-32-5; [(OEP)GaOAc]⁺, 109907-25-7; [(OEP)GaOAc]²⁺, 109907-35-9; [(OEP)GaF]²⁻, 109907-44-0; [(OEP)GaF]⁻, 109907-28-0; (OEP)GaF, 104453-21-6; [(OEP)GaF]⁺, 109907-27-9; [(OEP)GaF]²⁺, 109907-36-0; [(OEP)GaOH(H₂O)]²⁻, 109907-45-1; [(OEP)GaOH(H₂O)]⁻, 109907-30-4; (OEP)GaOH(H₂O), 109907-18-8; [(OEP)GaOH(H₂O)]⁺, 109907-29-1; [(OEP)GaOH(H₂O)]²⁺, 109907-37-1; (OEP)GaOAc(py), 109907-51-9; [(OEP)GaF(N-MeIm)]⁻, 109907-64-4; (OEP)GaF(N-MeIm), 109927-20-0; (OEP)GaF(py), 109907-52-0; (OEP)GaOH(py), 109907-54-2; [(OEP)GaOH(N-MeIm)]⁻, 109907-60-0; (OEP)GaOH(N-MeIm), 109907-53-1; [(OEP)Ga(N-MeIm)]⁻, 109907-63-3; (OEP)Ga(N-MeIm)₂, 109907-62-2; [(OEP)Ga(N-MeIm)₂]⁺, 109907-61-1; [(OEP)Ga(py)]⁻, 109907-69-9; (OEP)Ga(py)₂, 109907-67-7; [(OEP)Ga(py)₂]⁺, 109907-65-5.

(40) Nicholson, R. S.; Shain, I. *Anal. Chem.* 1964, 36, 706.

(41) See for review: Kadish, K. M. In *Iron Porphyrins, Part 2*; Lever, A. B. P., Gray, H. B., Eds.; Addison-Wesley: Reading, MA, 1983; pp 161–249.